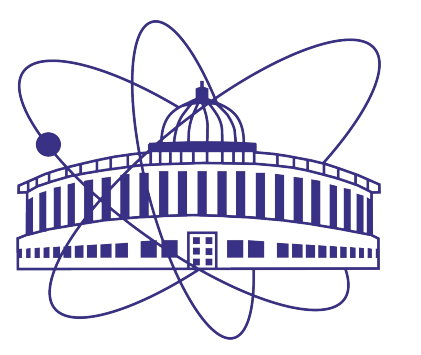
Feasibility study of the anisotropic flow measurements with fixed-target mode of the MPD experiment at NICA

P. Parfenov, M. Mamaev and A. Taranenko (JINR, NRNU MEPhI)

LXXV International Conference Nucleus-2025: Fundamental Problems and Applications 1-6 July 2025

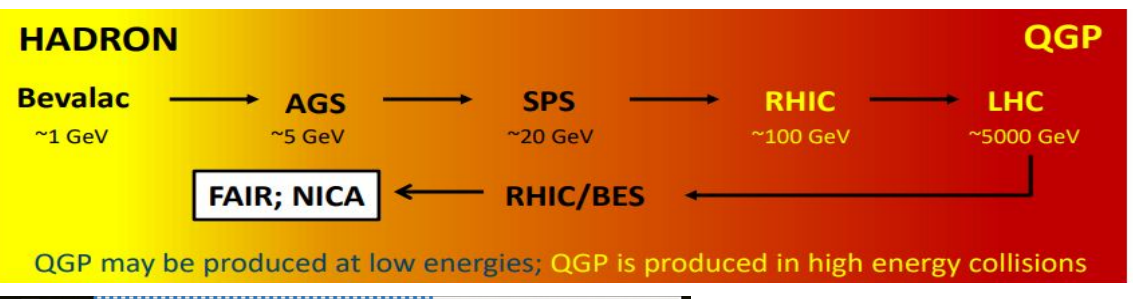




The research has been supported by the Ministry of Science and Higher Education of the Russian Federation, Project "New Phenomena in Particle Physics and the Early Universe" No. FSWU-2023-0073

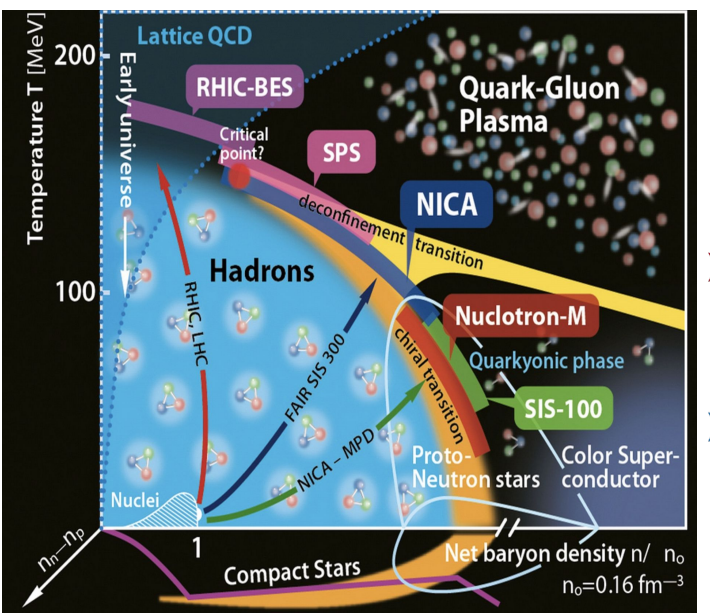


Relativistic heavy-ion collisions



1970s-2000s – nuclear equation of state (EoS), search for the quark-gluon plasma (QGP) $\underline{2005s}$ – QGP formation was observed at RHIC and it behaves as almost perfect liquid $\underline{2005-2010s}$ – LQCD predicts crossover phase transition at top RHIC and LHC (high T, $\mu_B \approx 0$)

Since 2010s – Beam energy scans to study QCD phase diagram: search for the 1st order phase transition and CEP at Intermediate T, high μ_B



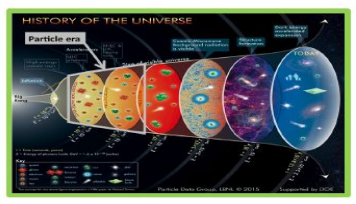
Relativistic heavy-ion collisions allows us to study QCD phase diagram

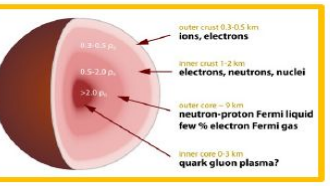
\triangleright High beam energies ($\sqrt{s_{NN}}$ >100 GeV):

- High T, $\mu_B \approx 0$
- Evolution of the early Universe

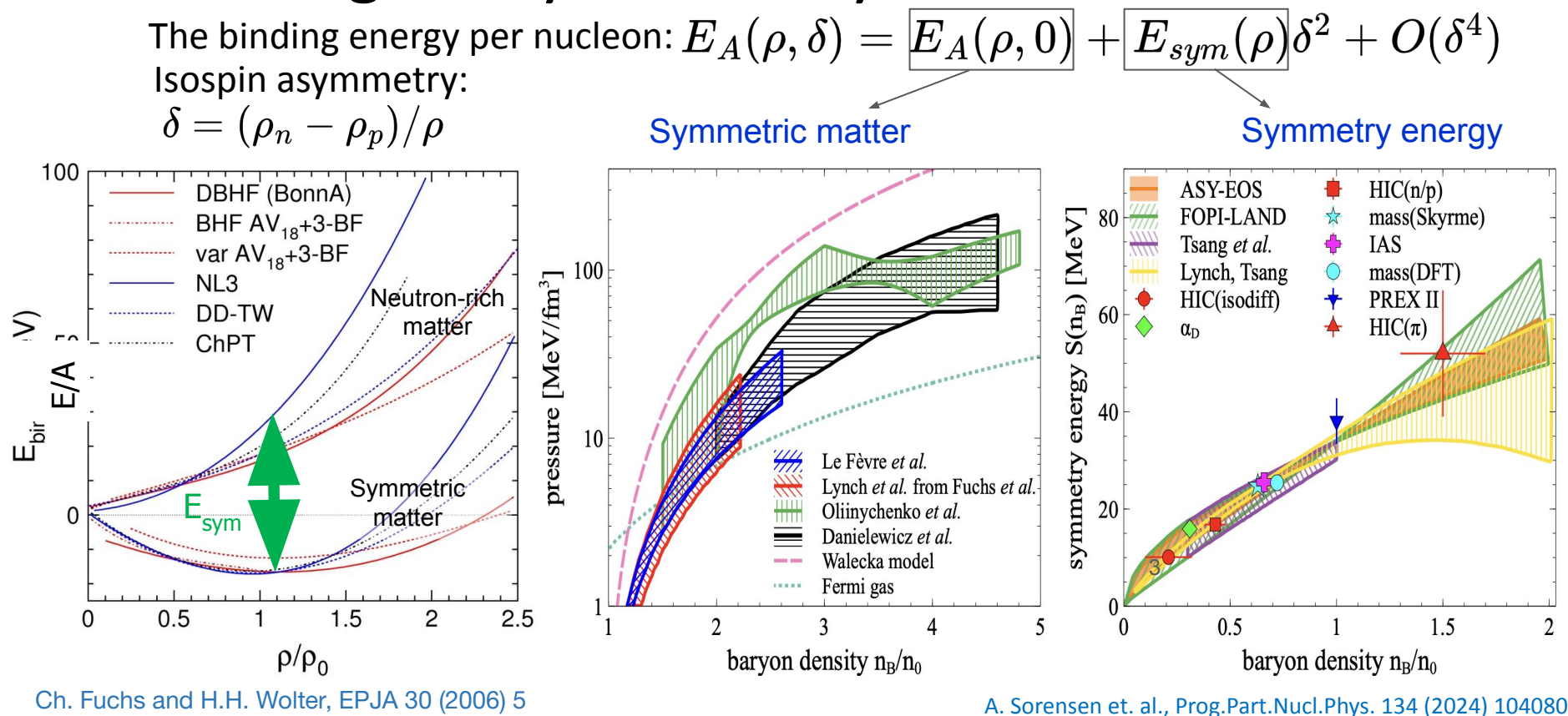
\triangleright Low beam energies (2.4< $\sqrt{s_{NN}}$ <11 GeV):

- Intermediate T, high μ_B
 - Inner structure of the compact stars, neutron star mergers



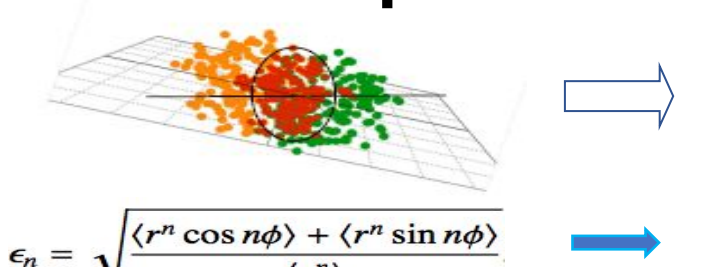


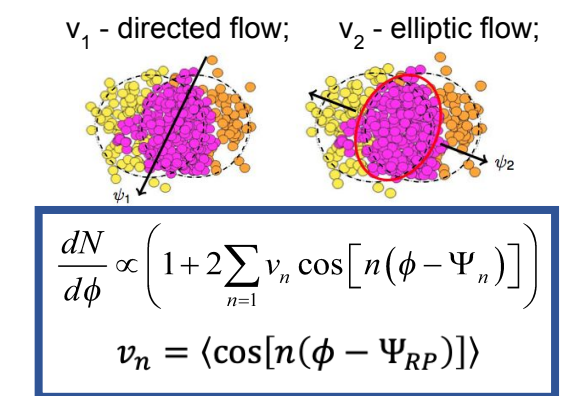
EOS for high baryon density matter



New data is needed to further constrain transport models with hadronic d.o.f.

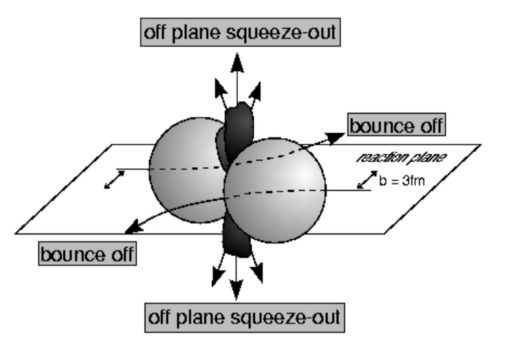
Anisotropic flow





Collision Energy √S_{NN} (GeV)

Initial eccentricity (and its attendant fluctuations) $\epsilon_{\rm n}$ drive momentum anisotropy ${\bf v}_{\rm r}$ with specific viscous modulation



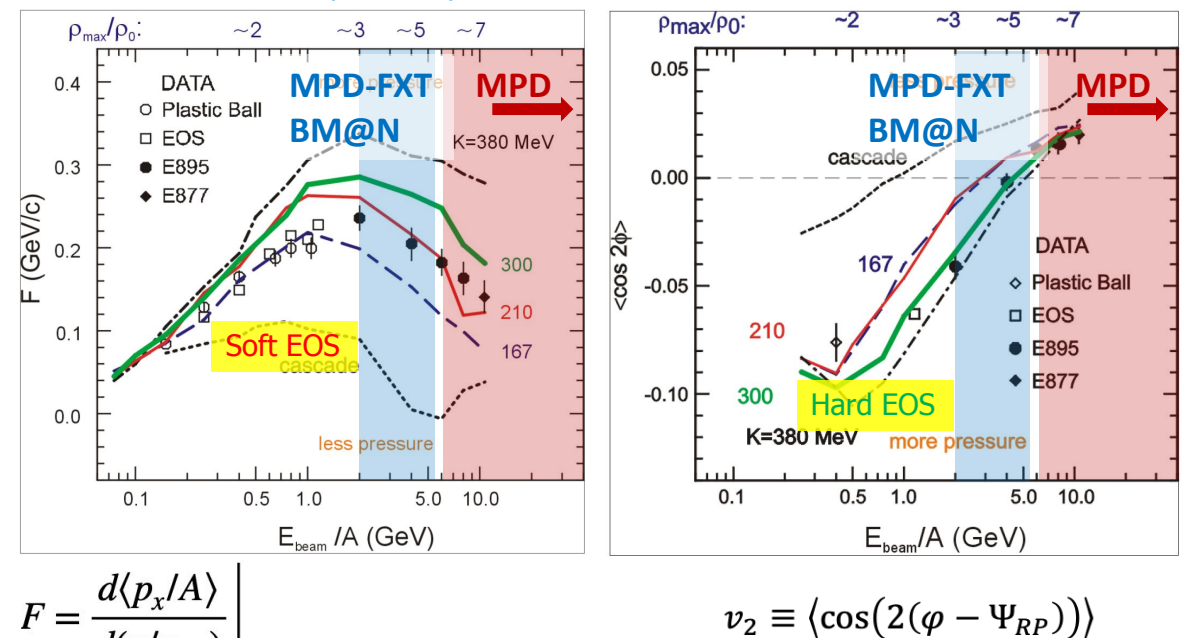
At Nuclotron-NICA:

Strong energy dependence of dv_1/dy and v_2 at $\sqrt{s_{NN}}$ =2-11 GeV Anisotropic flow at Nuclotron-NICA energies is a delicate balance between:

- I. The ability of pressure developed early in the reaction zone $(t_{exp} = R/c_s)$
- II. The passage time for removal of the shadowing by spectators $(t_{pass} = 2R/\gamma_{CM}\beta_{CM})$

Sensitivity of the collective flow to the EOS

P. Danielewicz, R. Lacey, W.G. Lynch, Science 298 (2002)



Anisotropic flow sensitive to the EoS **EoS** extraction: define incompressibility

$$K_0 = 9\rho^2 \frac{\partial^2(E_A)}{\partial \rho^2}$$

Discrepancy in the interpretation:

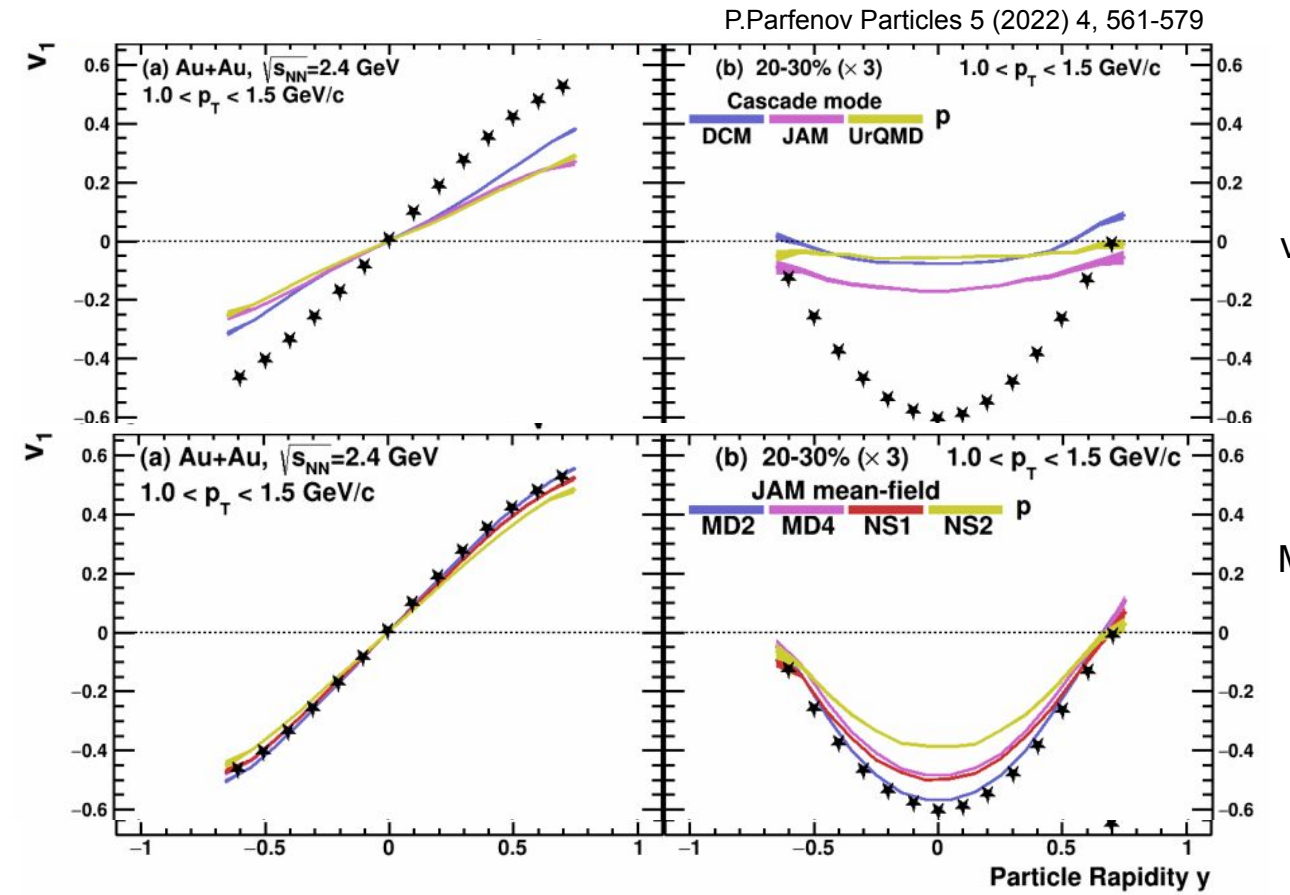
- v_1 suggests soft EoS ($K_0 \approx 210$ MeV)
- v_2 suggests hard EoS ($K_0 \approx 380$ MeV)

New measurements using new data and modern analysis techniques might address this discrepancy

Additional measurements are essential to clarify the previous results

 $v_2 \equiv \langle \cos(2(\varphi - \Psi_{RP})) \rangle$

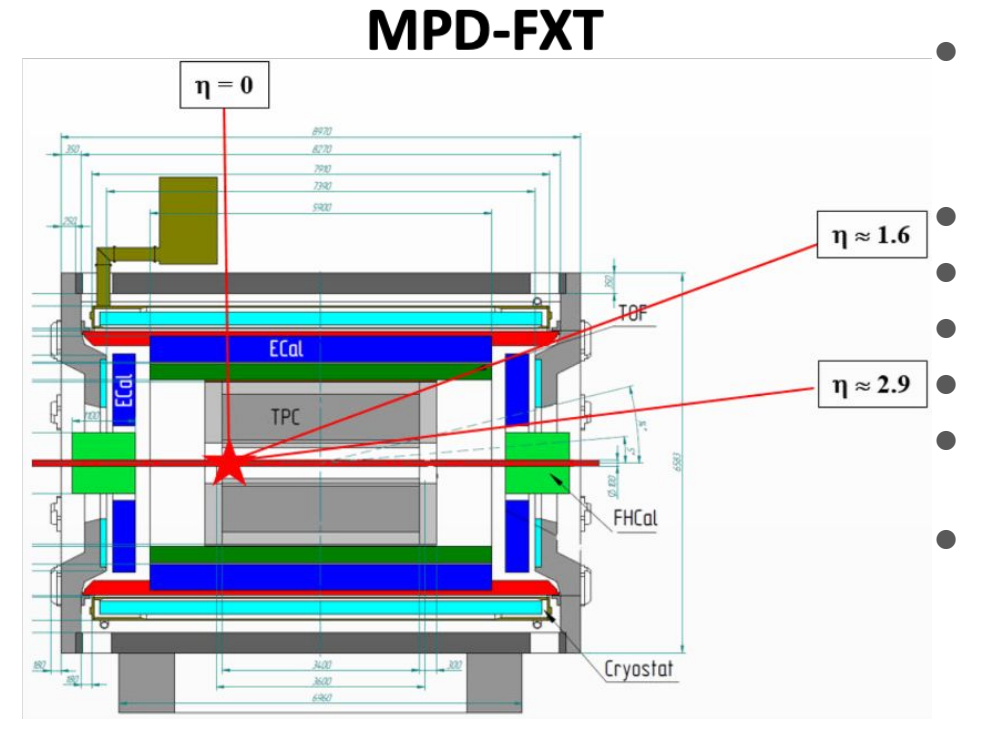
Selecting the model for the feasibility studies



Cascade models fail to reproduce v_n at low-energy heavy-ion collision

Mean field models reproduce the v_n rather well

MPD in Fixed-Target Mode (FXT)



Model used: UrQMD mean-field

- \circ Xe+W, E_{kin}=2.5 AGeV ($\sqrt{s_{NN}}$ =2.87 GeV)
- \circ Xe+Xe, E_{kin} =2.5 AGeV ($\sqrt{s_{NN}}$ =2.87 GeV)

Point-like target at z = -85 cm, y = 1 cm

GEANT4 transport

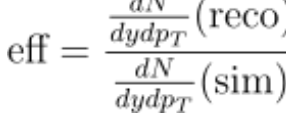
Multiplicity-based centrality determination

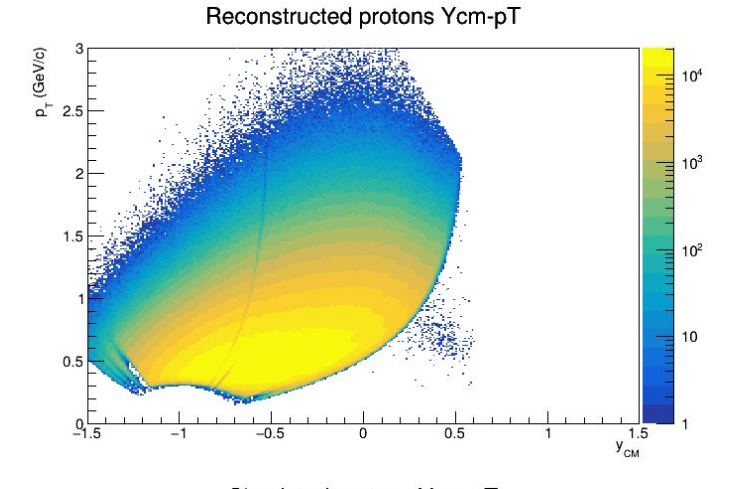
PID using information from TPC and TOF

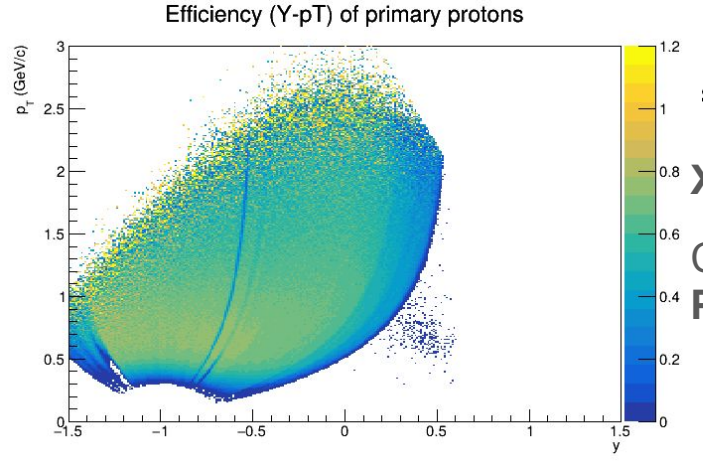
Primary track selection:

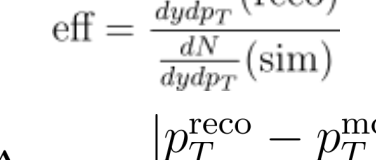
- o DCA<1 cm (protons) DCA<0.2 cm (pions)
- Track selection:
 - N_{hits}>27 (protons), N_{hits}>22 (pions)

(y-pt) distribution, efficiency and δpt (protons)







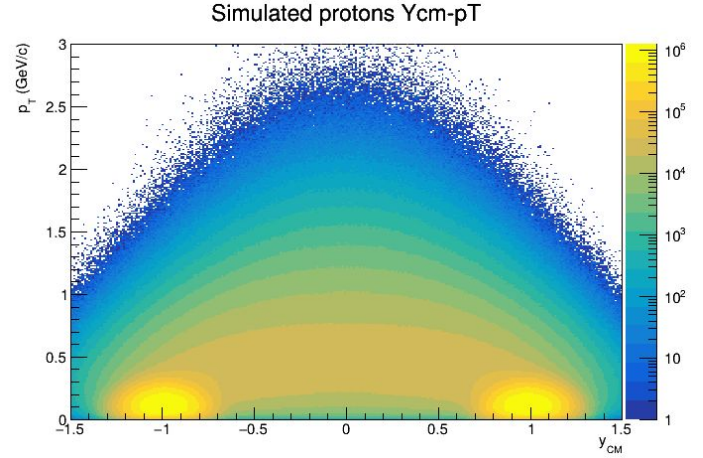


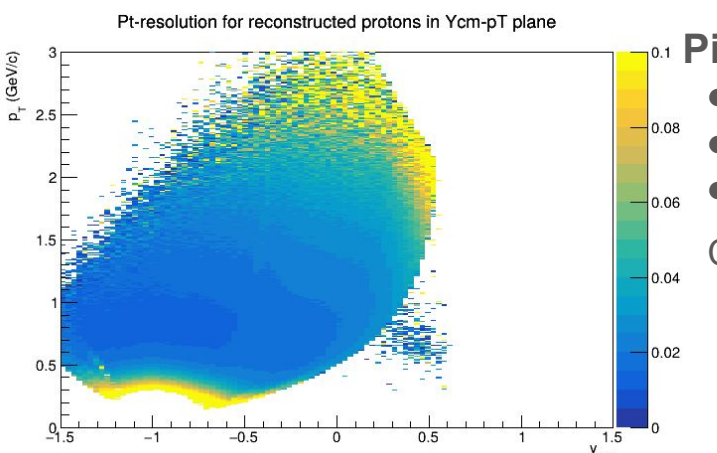
• Xe+W/Xe T=2.5A GeV

Cuts for reco tracks:

^{0.4} Protons:

- Nhits>27
- DCA< 1 cm
- PID (TPC+TOF)





on Pions:

- Nhits>22
- DCA< 0.2 cm
- PID (TPC+TOF)

Cuts for sim particles:

- PID (pdg code)
- Primary (motherId)

Flow vectors

From momentum of each measured particle define a u_n -vector in transverse plane:

$$u_n=e^{in\phi}$$

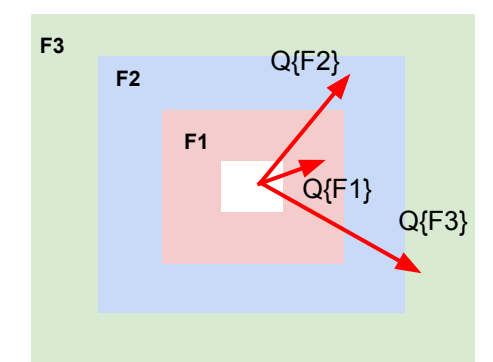
where ϕ is the azimuthal angle

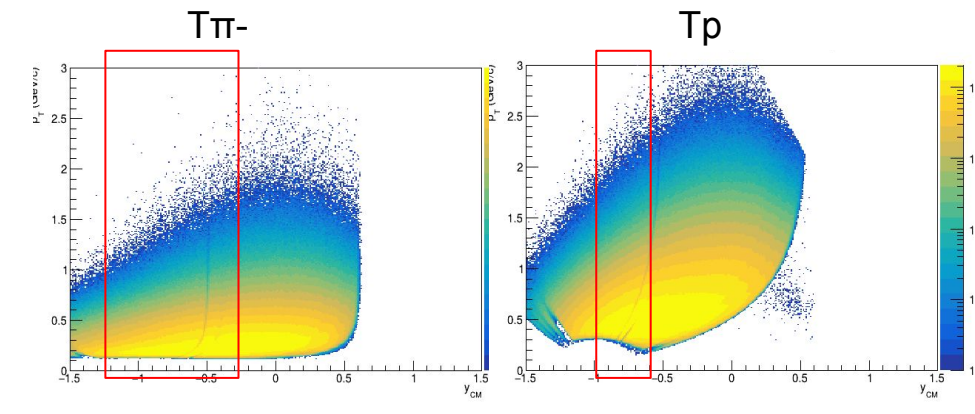
Sum over a group of u_n -vectors in one event forms Q_n -vector:

$$Q_n = rac{\sum_{k=1}^N w_n^k u_n^k}{\sum_{k=1}^N w_n^k} = |Q_n| e^{in\Psi_n^{EP}}$$

 Ψ_n^{EP} is the event plane angle

Modules of FHCal divided into 3 groups





Additional subevents from tracks not pointing at FHCal:

Tp: p; -1.0<y<-0.6;

Tπ: π-; -1.5<y<-0.2;

Flow methods for v_n calculation

Tested in HADES: M Mamaev et al 2020 PPNuclei 53, 277–281 M Mamaev et al 2020 J. Phys.: Conf. Ser. 1690 012122

Scalar product (SP) method:

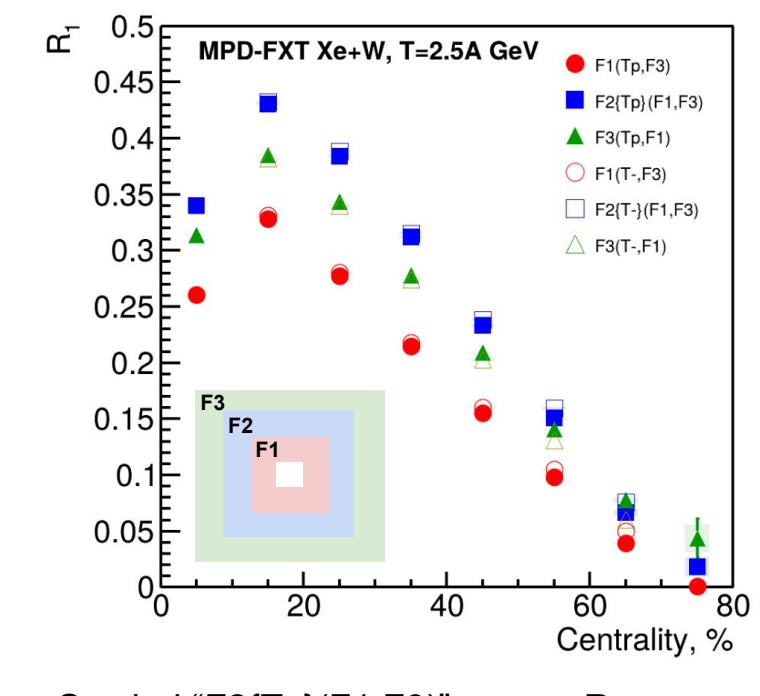
$$v_1 = rac{\langle u_1 Q_1^{F1}
angle}{R_1^{F1}} \qquad v_2 = rac{\langle u_2 Q_1^{F1} Q_1^{F3}
angle}{R_1^{F1} R_1^{F3}}$$

Where R₁ is the resolution correction factor

$$R_1^{F1} = \langle \cos(\Psi_1^{F1} - \Psi_1^{RP})
angle$$

Symbol "F2(F1,F3)" means R₁ calculated via (3S resolution):

$$R_1^{F2(F1,F3)} = rac{\sqrt{\langle Q_1^{F2}Q_1^{F1}
angle \langle Q_1^{F2}Q_1^{F3}
angle}}{\sqrt{\langle Q_1^{F1}Q_1^{F3}
angle}}$$

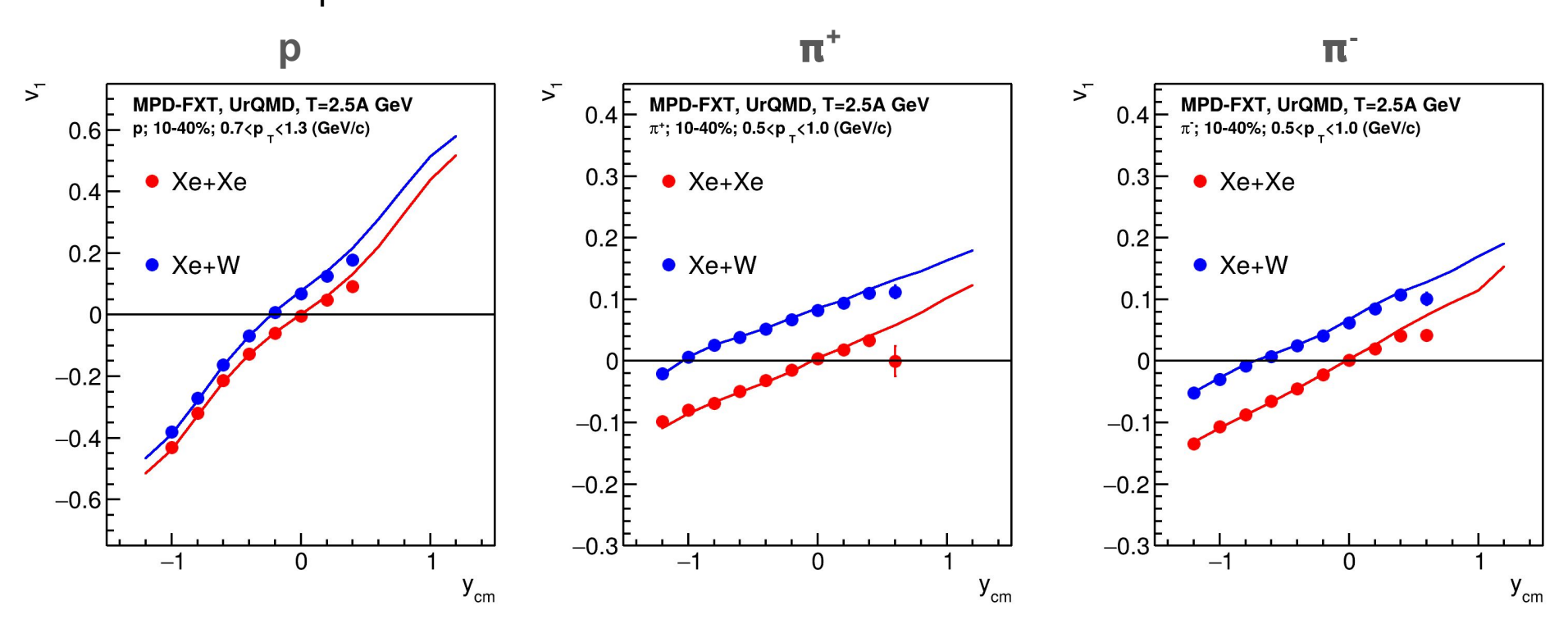


Symbol "F2{Tp}(F1,F3)" means R₁ calculated via (4S resolution):

$$R_1^{F2\{Tp\}(F1,F3)} = \langle Q_1^{F2}Q_1^{Tp}
angle rac{\sqrt{\langle Q_1^{F1}Q_1^{F3}
angle}}{\sqrt{\langle Q_1^{Tp}Q_1^{F1}
angle \langle Q_1^{Tp}Q_1^{F3}
angle}}$$

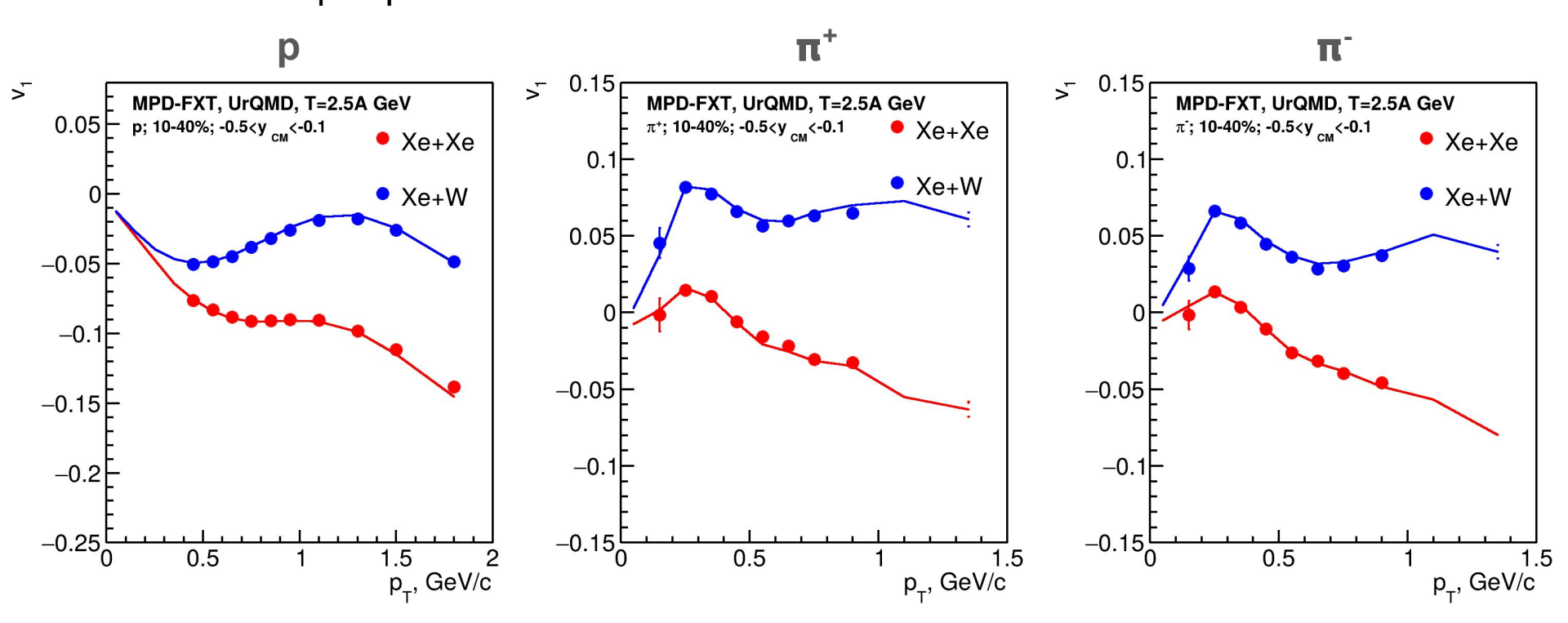
Results: $v_1(y)$

markers - reco; lines - model



Good agreement for protons and pions for y<0.5

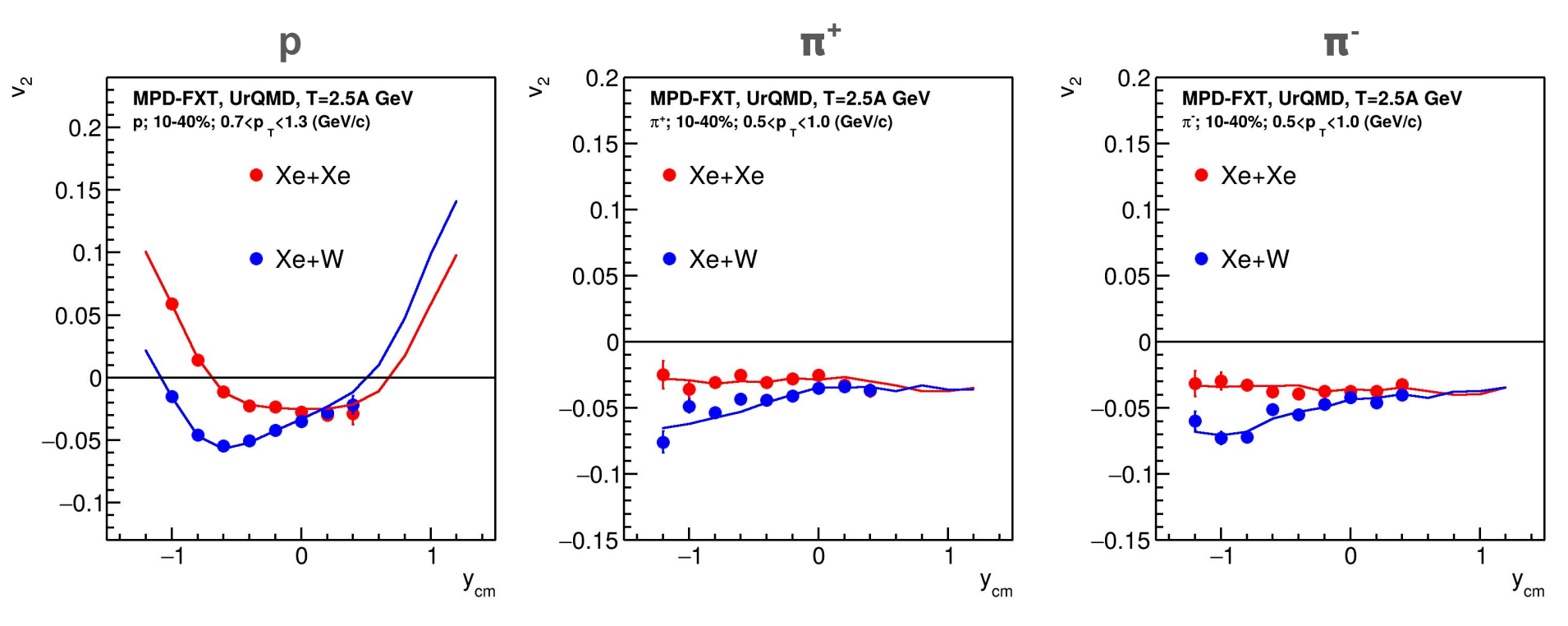
Clear shift in $v_1(y_{cm})$ for Xe+W - preferential deflection of the participants



Good agreement for protons and pions

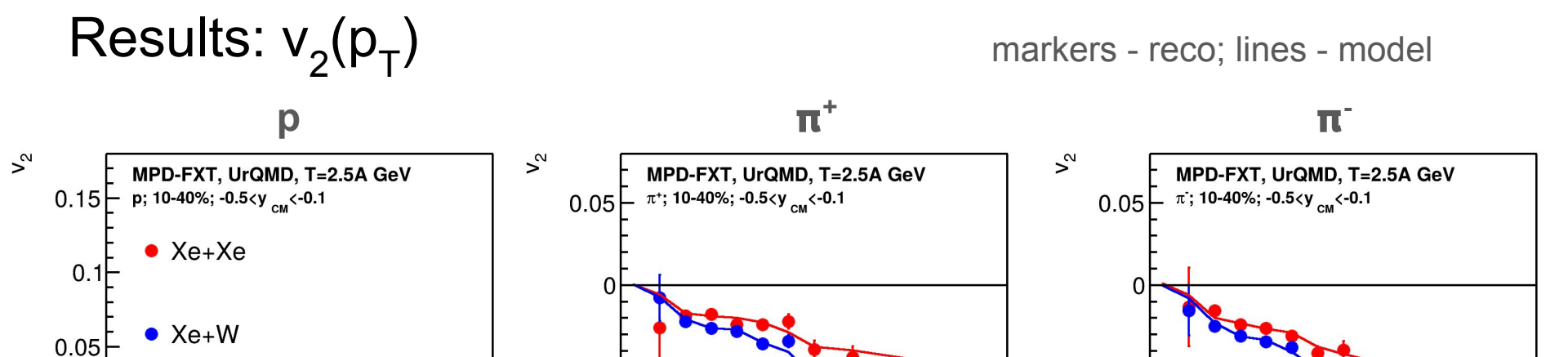
Results: $v_2(y)$

markers - reco; lines - model



Good agreement for protons and pions for y<0.5

Asymmetric $v_2(y_{cm})$ dependence for Xe+W



-0.05

-0.1

-0.15

Xe+Xe

Xe+W

0.5

-0.05

-0.1

-0.15

-0.05

-0.1

0.5

1.5

p_T, GeV/c

Xe+Xe

Xe+W

Good agreement for protons and pions

 p_{τ} , GeV/c

0.5

1.5 p_T, GeV/c

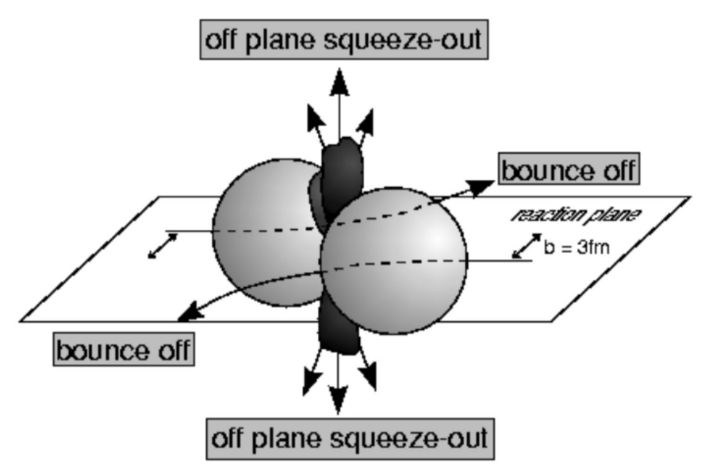
Summary

- Feasibility study shows that MPD-FXT configuration is capable of the precise differential measurements of the anisotropic flow coefficients using realistic centrality determination and particle identification techniques
- Directed and elliptic flow of protons and pions were measured for at T=2.5A GeV ($\sqrt{s_{NN}}$ = 2.87 GeV):
 - Good agreement between reconstructed and model data within corresponding acceptance windows for protons and pions
- Two colliding systems (Xe+W, Xe+Xe) were compared:
 - There is a clear shift in v₁(y_{cm}) for Xe+W, consistent with the participant deflection dynamics in asymmetric systems;
 - Noticeable v₂(y_{cm}) dependence in both systems, with characteristically asymmetric behavior for Xe+W collisions

Thank you for your attention!

Backup

Anisotropic flow & spectators



The azimuthal angle distribution is decomposed in a Fourier series relative to reaction plane angle:

$$ho(arphi-\Psi_{RP})=rac{1}{2\pi}(1+2\sum_{n=1}^{\infty}v_n\cos n(arphi-\Psi_{RP}))$$

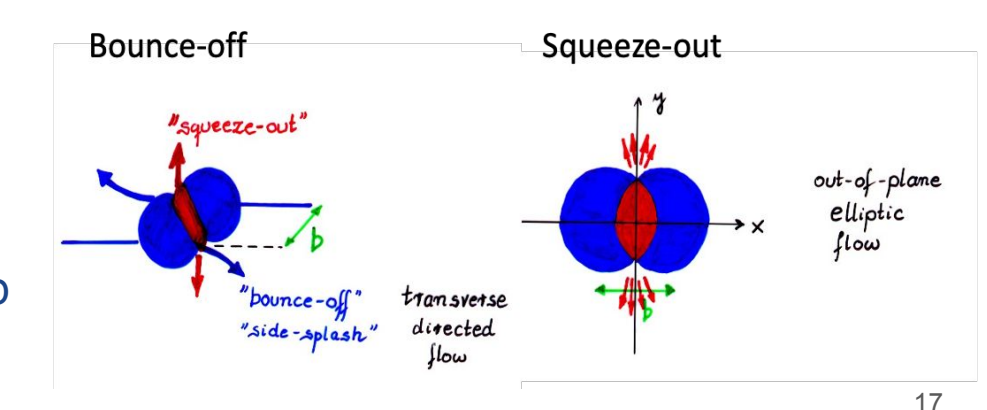
Anisotropic flow:

$$v_n = \langle \cos \left[n (arphi - \Psi_{RP})
ight]
angle$$

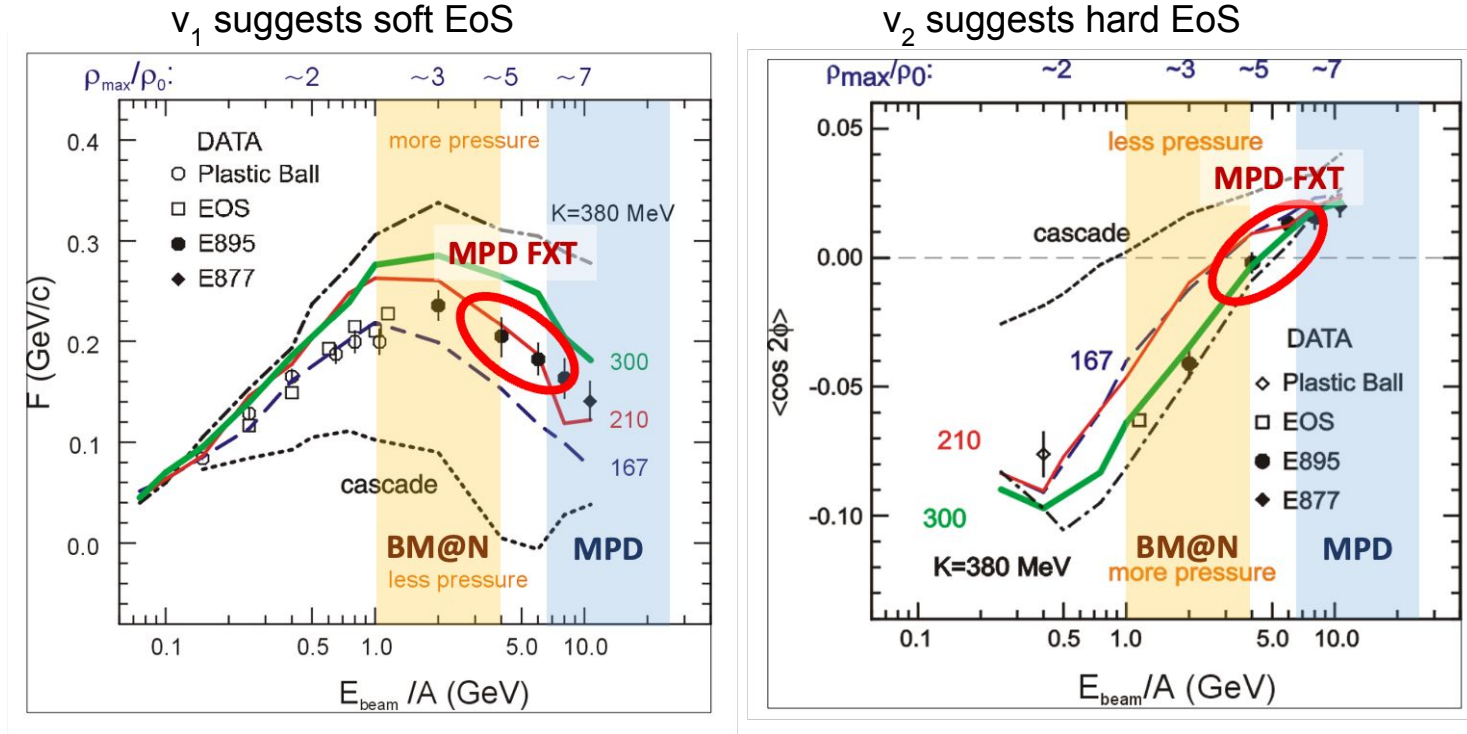
 v_1 - directed flow, v_2 - elliptic flow

Anisotropic flow is sensitive to:

- ➤ Compressibility of the created matter $\left(t_{exp} = R/c_s, \ c_s = c\sqrt{dp/d\varepsilon}\right)$ ➤ Time of the interaction between overlap
- Time of the interaction between overlap region and spectators $(t_{pass} = 2R/\gamma_{CM}\beta_{CM})$

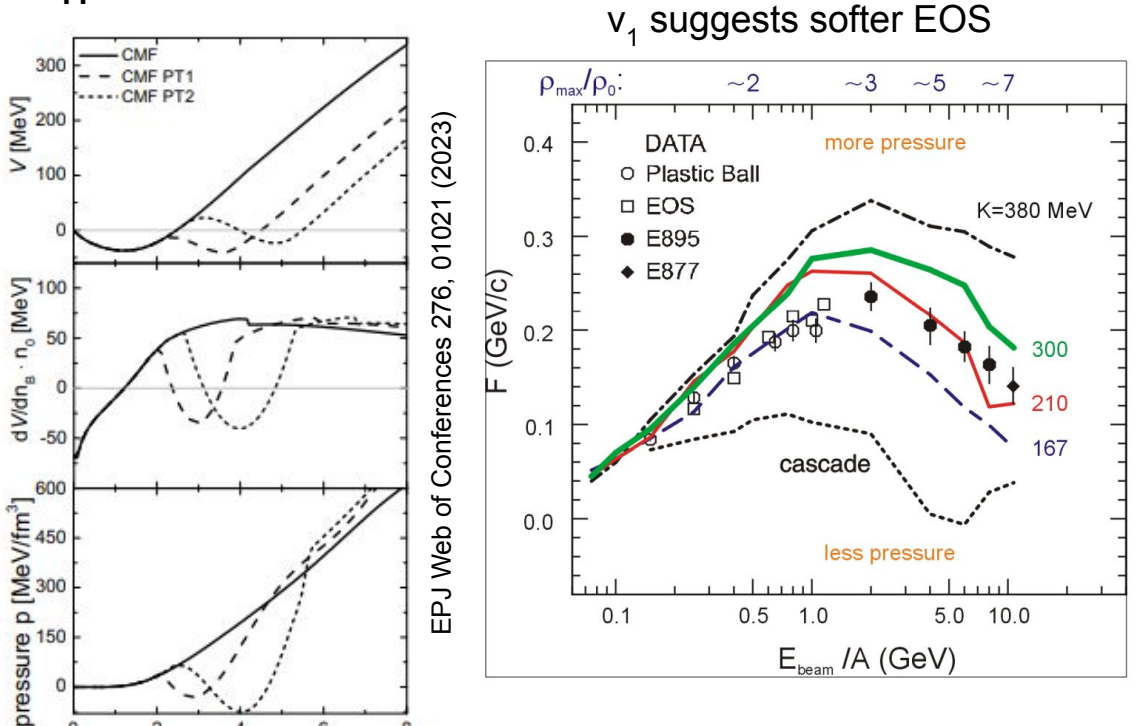


v_n at Nuclotron-NICA energies



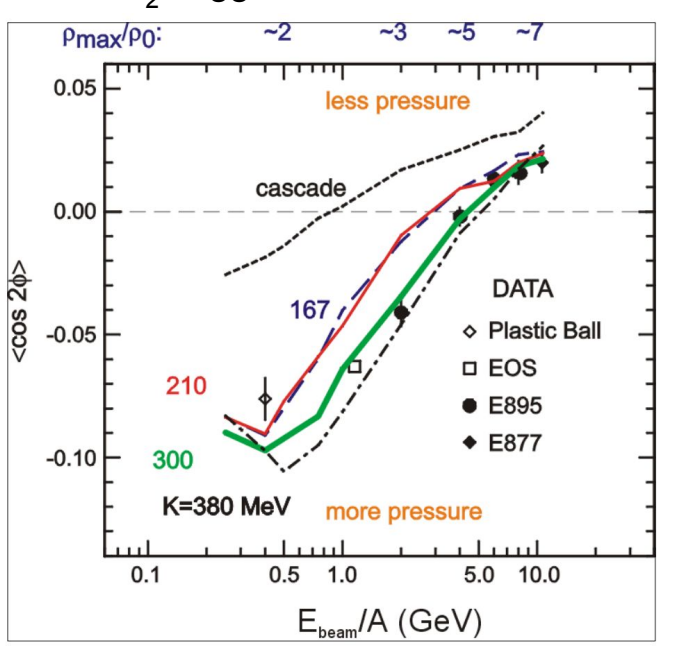
- v_n results from the E895 experiment are ambiguous:
 - v₁ suggests soft EoS and v₂ suggests hard EoS
- Additional experimental data are required to address this discrepancy

v_n as a function of collision energy



P. DANIELEWICZ, R. LACEY, W. LYNCH 10.1126/science.1078070

v₂ suggests harder EOS



Describing the high-density matter using the mean field Flow measurements constrain the mean field

Discrepancy is probably due to non-flow correlations

The Bayesian inversion method (Γ-fit)

Relation between multiplicity N_{ch} and impact parameter b is defined by the fluctuation kernel:

 $P(N_{ch}|c_b) = \frac{1}{\Gamma(k(c_b))\theta^k} N_{ch}^{k(c_b)-1} e^{-n/\theta} \qquad \frac{\sigma^2}{\langle N_{ch} \rangle} = \theta \approx const, \ k = \frac{\langle N_{ch} \rangle}{\theta}$ $c_b = \int_0^b P(b')db' - \text{centrality based on impact parameter}$

Mean multiplicity as a function of c_h can be defined as follows:

$$\left\langle N_{ch} \right\rangle = N_{knee} \exp \left(\sum_{j=1}^{3} a_{j} c_{b}^{j} \right) \quad N_{knee}, \, \theta, \, a_{j} \,$$
 - 5 parameters

Fit function for N_{ch} distribution: b-distribution for a given N_{ch} range:

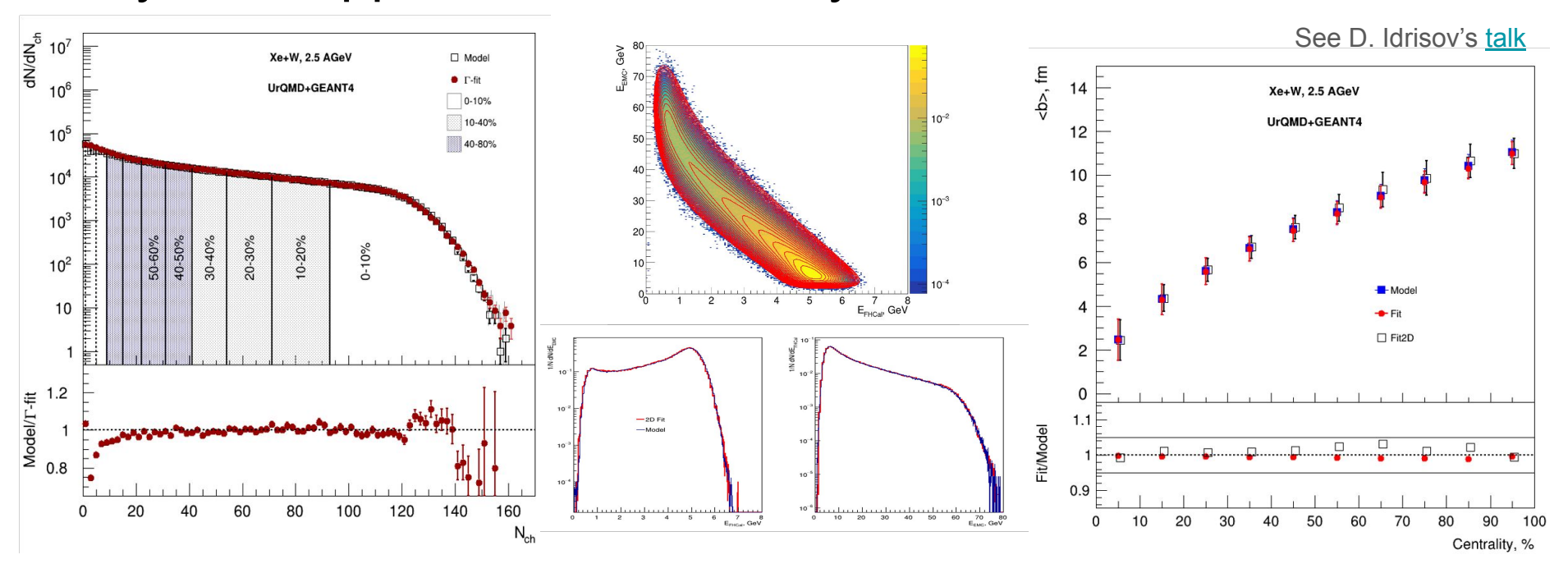
$$P(N_{ch}) = \int_0^1 P(N_{ch}|c_b)dc_b \quad P(b|n_1 < N_{ch} < n_2) = P(b) \frac{\int_{n_1}^{n_2} P(N_{ch}|b)dN_{ch}}{\int_{n_1}^{n_2} P(N_{ch})dN_{ch}}$$

2 main steps of the method:

Fit experimental (model) distribution with P(N)

Construct P(b|E) using Bayes' theorem: P(b|N) = P(b)P(N|b)/P(N)

Bayesian approach for centrality in MPD-FXT



Both 1D and 2D bayesian inversion techniques can be employed for centrality determination

We can suppress auto-correlation effects by using energy from EMC (with specific selection) it is important for fluctuation studies (cumulants of net-proton, kaons, etc.)

PID procedure

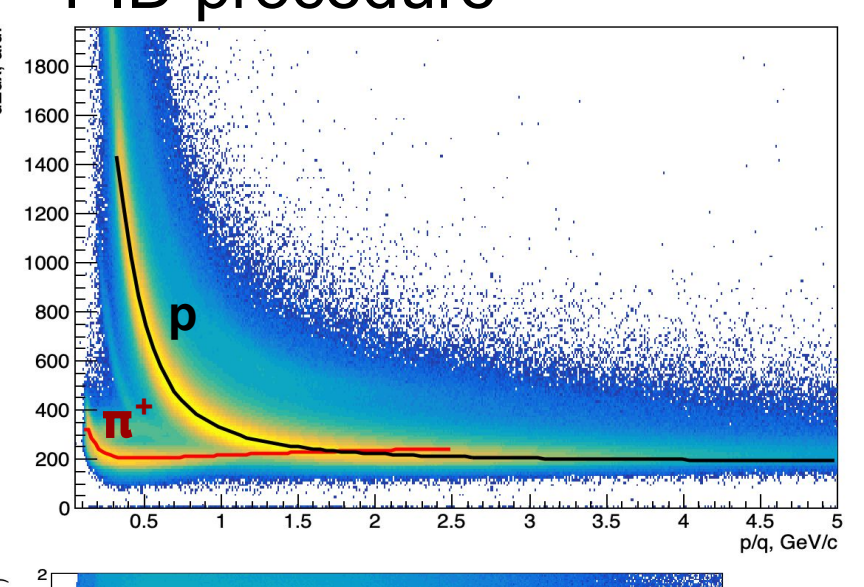
W. Blum, W. Riegler, L. Rolandi, Particle Detection with Drift

Chambers (2nd ed.), Springer, Verlag (2008)

Fit dE/dx distributions with Bethe-Bloch parametrization:

$$\begin{split} f(\beta\gamma) &= \frac{p_1}{\beta^{p_4}} \left(p_2 - \beta^{p_4} - \ln \left(p_3 + \frac{1}{(\beta\gamma)^{p_5}} \right) \right) \\ \beta^2 &= \frac{p^2}{m^2 + p^2}, \beta\gamma = \frac{p}{m} \quad \textbf{\textit{p}}_{\it{i}} \text{ - fit parameters} \end{split}$$

Fit $(dE/dx - f(\beta y))/f(\beta y)$ with gaus in the slices of p/q and get $\sigma_{n}(dE/dx)$

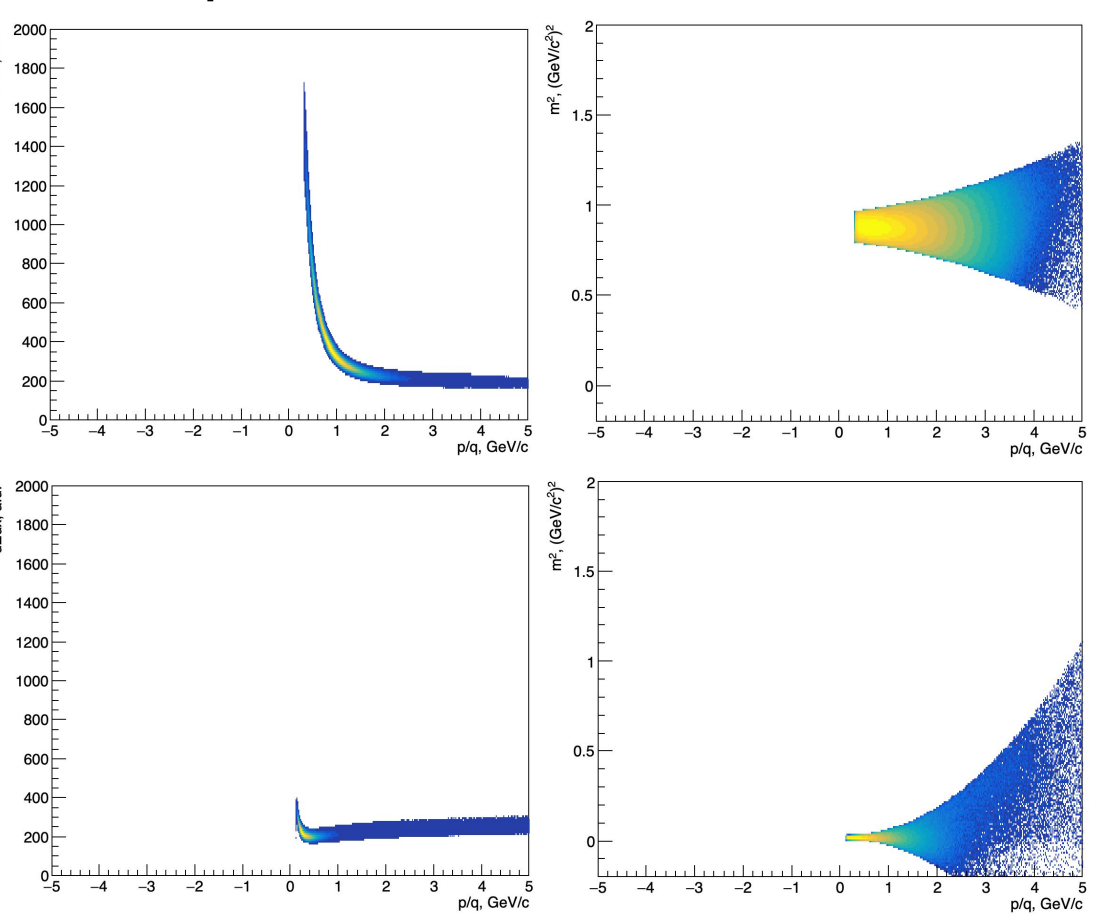


p/q, GeV/c

Fit m² with gaus in the slices of p/q and get $\sigma_{p}(m^{2})$

 $(dE/dx,m)\rightarrow (x,y)$ coordinates for PID: $x_p = \frac{(dE/dx)^{meas} - (dE/dx)_p^{fit}}{(dE/dx)_p^{fit} \sigma_p^{dE/dx}}, \ y_p = \frac{m^2 - m_p^2}{\sigma_p^{m^2}}$

PID procedure: Results



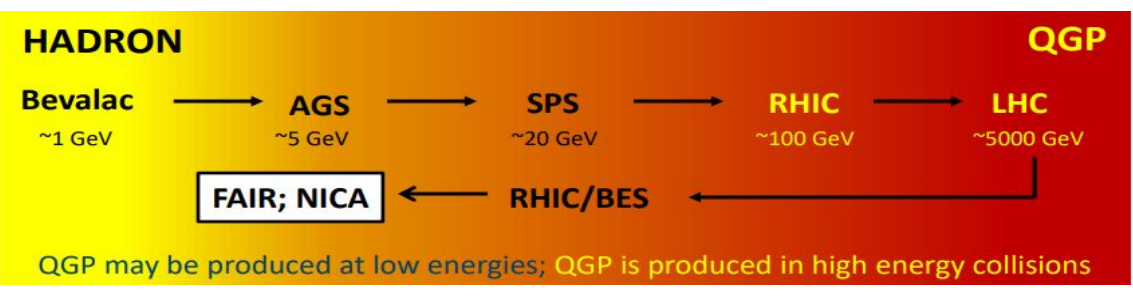
$$x_p = \frac{(dE/dx)^{meas} - (dE/dx)_p^{fit}}{(dE/dx)_p^{fit} \sigma_p^{dE/dx}}$$
$$y_p = \frac{m^2 - m_p^2}{\sigma_p^{m^2}}$$

Protons:
$$\sqrt{x_p^2 + y_p^2} < 2, \sqrt{x_\pi^2 + y_\pi^2} > 3$$

Pions (
$$\pi^+$$
):
$$\sqrt{x_\pi^2 + y_\pi^2} < 2, \sqrt{x_p^2 + y_p^2} > 3$$

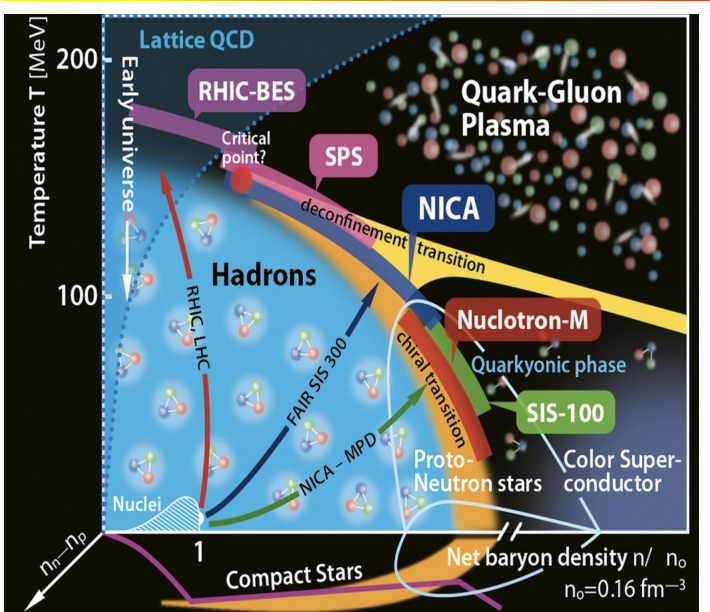
Pions (π^{-}) : charge<0

Relativistic heavy-ion collisions



1970s-2000s – nuclear equation of state (EoS), search for the quark-gluon plasma (QGP) 2005s – QGP formation was observed at RHIC and it behaves as almost perfect liquid 2005-2010s – LQCD predicts crossover phase transition at top RHIC and LHC (high T, $\mu_B \approx 0$)

Since 2010s – Beam energy scans to study QCD phase diagram: search for the 1st order phase transition and CEP at Intermediate T, high μ_B



Relativistic heavy-ion collisions allows us to study QCD phase diagram

- \triangleright High beam energies ($\sqrt{s_{NN}}$ >100 GeV):
 - High T, $\mu_R \approx 0$
 - · Evolution of the early Universe

24

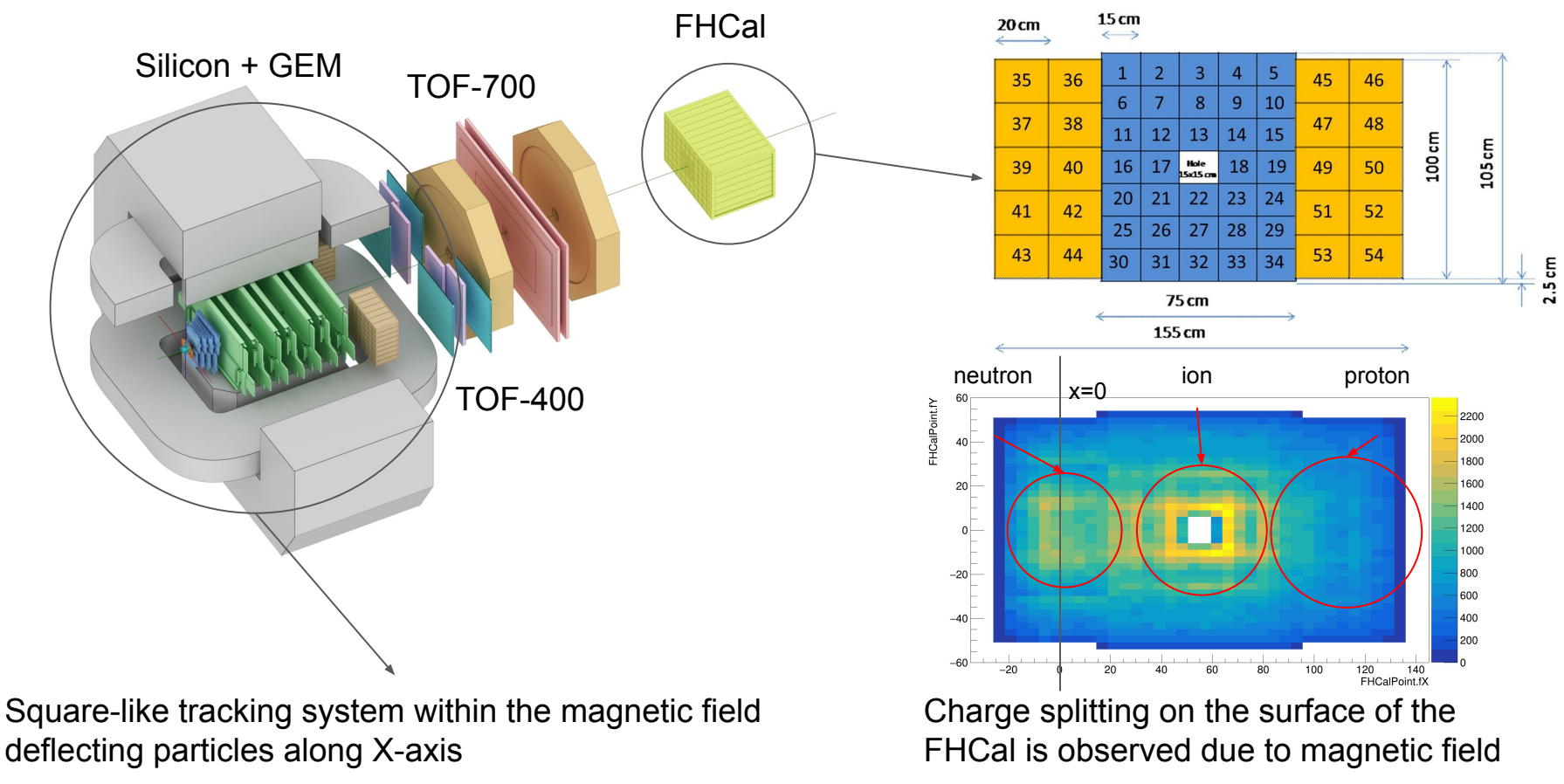
- \triangleright Low beam energies (2.4< $\sqrt{s_{NN}}$ <11 GeV):
 - Intermediate T, high μ_B
 - Inner structure of the compact stars, neutron star mergers



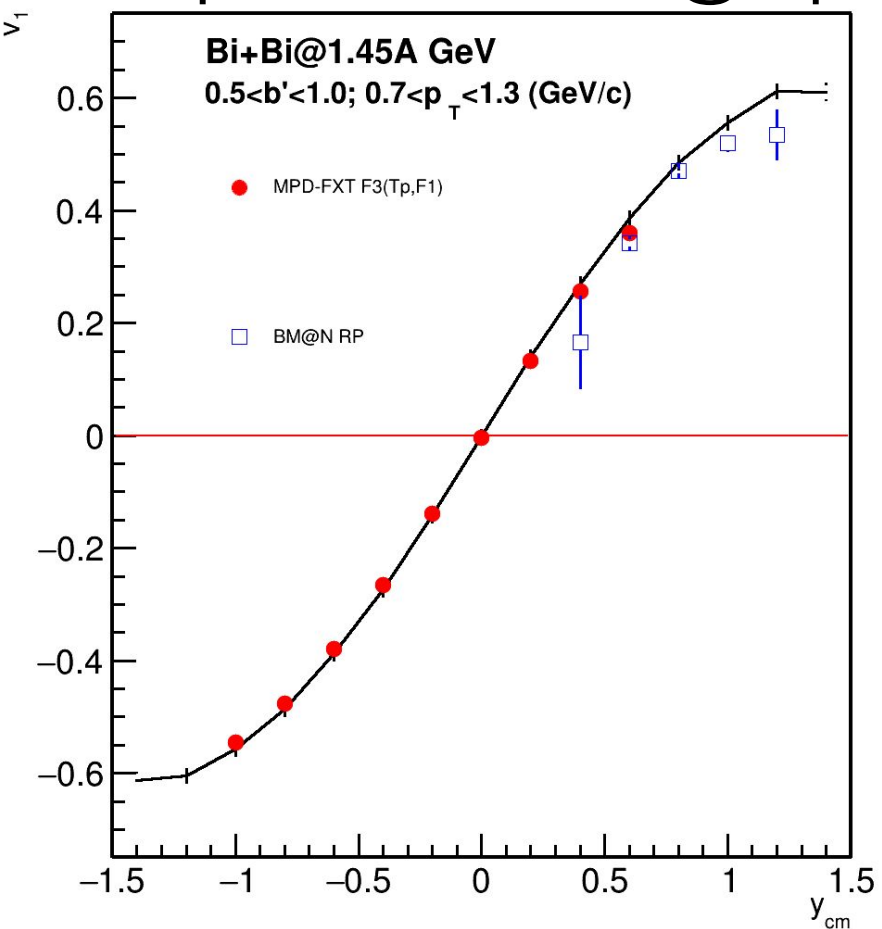


22.10.2024 ICPPA-2024

The BM@N experiment (GEANT4 simulation for RUN8)



Comparison with BM@N performance



BM@N TOF system (TOF-400 and TOF-700) has poor midrapidity coverage at $\sqrt{s_{NN}}$ = 2.5 GeV

- One needs to check higher energies ($\sqrt{s_{NN}} = 3$, 3.5 GeV)
- More statistics are required due to the effects of magnetic field in BM@N:
 - Only "yy" component of <uQ> and <QQ> correlation can be used

Despite the challenges, both MPD-FXT and BM@N can be used in v_n measurements:

- To widen rapidity coverage
- To perform a cross-check in the future